Hindawi
International Journal of RF and Microwave Computer-Aided Engineering
Volume 2023, Article ID 1319502, 6 pages
https://doi.org/10.1155/2023/1319502

Research Article

A K-Band Series-Fed WR42 Waveguide Horn Array with Beam Squint Reduction through Shunt Delay Sections

Alexander Simonovic and Tinus Stander

Department of EEC Engineering, University of Pretoria, Gauteng, South Africa

Correspondence should be addressed to Alexander Simonovic; alexander.simonovic@tuks.co.za

Received 18 November 2022; Revised 9 April 2023; Accepted 17 April 2023; Published 23 May 2023

Academic Editor: Arpan Desai

Series feeds are commonly used in antenna arrays because of their compact size and low loss compared to corporate feeds but typically feature beam squint over wide bandwidths. This work proposes a series-fed waveguide horn array with reduced beam squint by introducing synthesized time delay sections between the horns and the feed line. The array, implemented in a WR42 waveguide, achieves 1.53° beam squint over a 4 GHz operating band, compared to 10.52° for a reference design without time delay compensation.

1. Introduction

In antenna applications where high directivity is required over broad bandwidths, such as satellite communications and point-to-point links, arrays with corporate feed networks are commonly used because the feed network preserves equal phases at all output ports over wide bandwidths [1]. In contrast, series-fed arrays exhibit beam squint over wide bandwidths [2] due to the difference in propagation path length between the port and the array elements [2–4], which limit their value in next-generation broadband applications. Series feeds do present several advantages over corporate feeds, one of which is greater flexibility in array design as array sizes are not limited to $2n$ elements. Series feeds can also be designed to be more compact and can achieve higher efficiencies [5–7], which has motivated research into the solution of the beam squint problem. Beam squint in leaky wave antennas is usually overcome with a compensation lens at the output of the antenna that corrects the beam by squinting the beam in the opposite direction [8, 9]. These lenses increase the size of the antenna assembly and complicate construction. A classical method to address the problem is to implement true time delay beamforming with RF photonics [3], where the RF signal between the feed branch and radiator is transduced to optical fibre and the delay is controlled by optical means. While this is a flexible and effective method to control the beam, it requires substantial support electronics (including RF-to-laser transducers) which increases cost and complexity. Another potential solution is the inclusion of negative group delay (NGD) circuits in the feedline to create a superluminal or negative phase velocity (depending on steering angle) in the feedline [10, 11]. The inclusion of NGD circuits significantly complicates the construction of the array, limits the operating bandwidth, and introduces unwanted nonlinearity, noise, and potential instability in the system [2]. The solution also requires theoretically infinite phase velocity for a perfectly broadside steered beam. A passive solution to beam squint has been presented, whereby time delay sections of varying delays are inserted between the feedline and the array antennas to equalize the total amount of time delay between the array feed port and the individual radiators. The advantage with this approach is that no active circuitry is needed in the feedline, while still having a beam which has a constant direction. This work extends on previous efforts [1] by demonstrating, for the first time, a waveguide implementation of the principle suitable for K-band satcom applications. We demonstrate that, by adding synthesized sinusoidal delay sections between the series feed waveguide and the radiators, the beam squint over a wide bandwidth

can be reduced substantially while preserving the linear arrangement of radiators in the array.

2. Array Design

The four-element antenna was designed to operate in the K-band centred at 22.5 GHz with a broadside beam. The array is made up of T-junction power dividers, sinusoidal time delays, waveguide horn antennas, and a straight section of a WR42 waveguide. Waveguide horns were selected as radiators for their ease of printing, wide bandwidth, and finite directivity (which is required to suppress array grating lobes), though the concept demonstrated here may be applied to other types of radiators as well. Figure 1 shows a diagram of the antenna array when assembled. The power dividers are reactive T-junction power dividers [12], using an inductive iris and a septum to control the power split between the two output ports. The feed line was assembled by cascading three T-junction sections, with an E-plane bend used to feed the fourth branch. 10.1 dBi gain horns of aperture 15.24×19.47 mm and length 37.25 mm were used as radiators.

For peak directivity, the radiators were required to be spaced at 0.9 λ or 11.9 mm, which left no space for any of the horns to flare out. The spacing was adjusted for the next peak in directivity, leading to a spacing of 22.5 mm. This has the disadvantage that grating lobes are moved towards the main lobe. Considering that the array is a proof-of-concept design to demonstrate anti-beam squint properties, this was not seen as a major disadvantage. Reduction of the grating lobes was achieved by the patterns of the individual horn antennas.

2.1. Time Delay Sections. The challenge in the design of the delay sections was to ensure broadband equal time delay between the array feed port and the individual radiators, despite the dissimilar physical distance. To this end, sinusoidal time delay sections [13] were implemented, selected for their suitability to additive manufacturing. These sections have no hanging edges in the waveguide interior, preventing the need for internal support structures and the associated protrusions and roughness after removal of the supports. The top and bottom walls of the time delay sections follow a sinusoidal pattern (Figure 2) extending between ports with cosine shaping extending for 3 periods (16.67 mm) from the input and output ports. The delay is controlled by varying the period and amplitude of the sinusoidal pattern. Uniform sinusoids were used, as nonuniform sinusoidal corrugations have transmission magnitude filtering properties [14] which are undesired in this application. The time delay sections all have a fixed length of 100 mm to effect a linear array arrangement (Figure 1). A straight WR42 waveguide section feeds the final branch, while the delays preserve equal time delay at the radiators while considering the delay effect of the T-junctions as well. These delays were then tuned in a full-wave simulation, with no excitation of higher-order modes observed at the simulated ports.

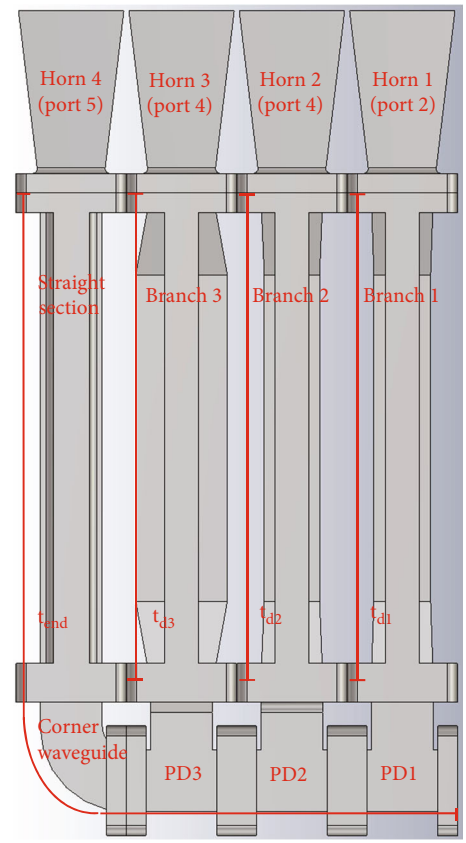

FIGURE 1: Annotated top-down view of the array antenna. Input of the antenna is on the bottom right and is referred to as port 1.

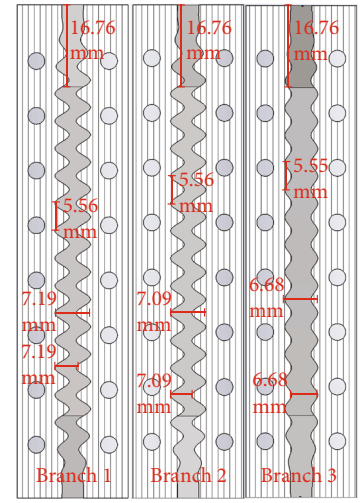

FIGURE 2: Section view showing the sinusoidal corrugation of the time delay sections.

3. Fabrication

The CAD files used to print parts were exported directly from those simulated in CST Studio Suite 2022. The waveguide parts were manufactured using SLA printing on a Form Lab Form 3 [15] using the manufacturer's white resin. The parts were then silver plated using a modified Tollens reaction [16]. This is a simple electroless plating reaction

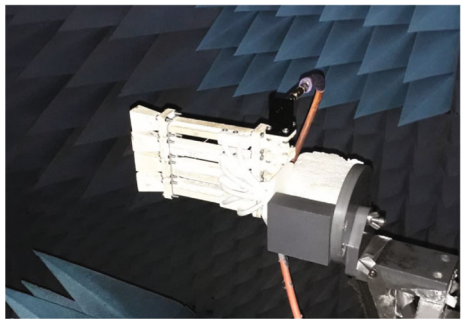

Figure 3: Antenna array on the measurement pedestal.

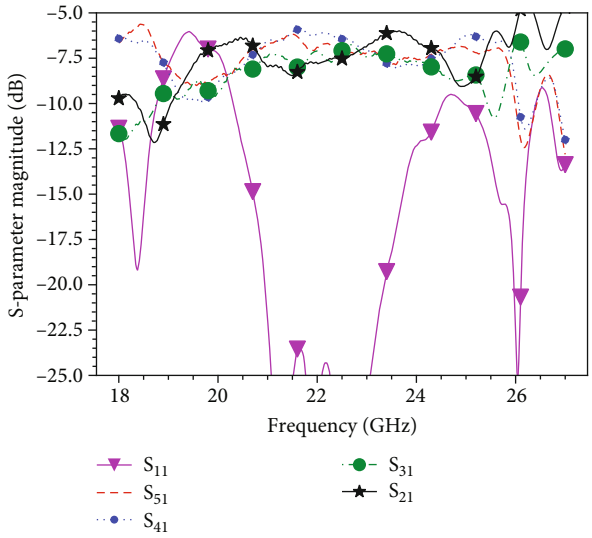

Figure 4: Measured S21 of the feed network.

that requires silver nitrate, ammonium hydroxide, sodium hydroxide, and dextrose, but no hazardous etching agents. The total manufacturing for the array was below 230 USD. The antenna that was made from individual parts is then assembled to produce the final array. This was done so the performance of the individual parts could be verified [17]. A reference design was also assembled for comparison, with the three delay line sections all replaced with straight waveguide sections, to measure the beam squint of a conventional array. This design represents the current state-of-the-art in series-fed waveguide array design that does not require lenses, reflectors, RF photonics, or other active circuitry. The standard array is referred to as the uncompensated array in this work while the compensated array uses time delay sections to compensate for the beam squint. The manufacturing process is discussed in more detail elsewhere [17, 18].

4. Experimental Results

The array was measured in a compact range (shown in Figure 3), with measurements taken at 500 MHz increments from 18 to 27 GHz across 360° azimuth and elevation angles. Boresight gain was also measured from 18 to 27 GHz. The array feed network was measured on an Anritsu MS6467A vector network analyser.

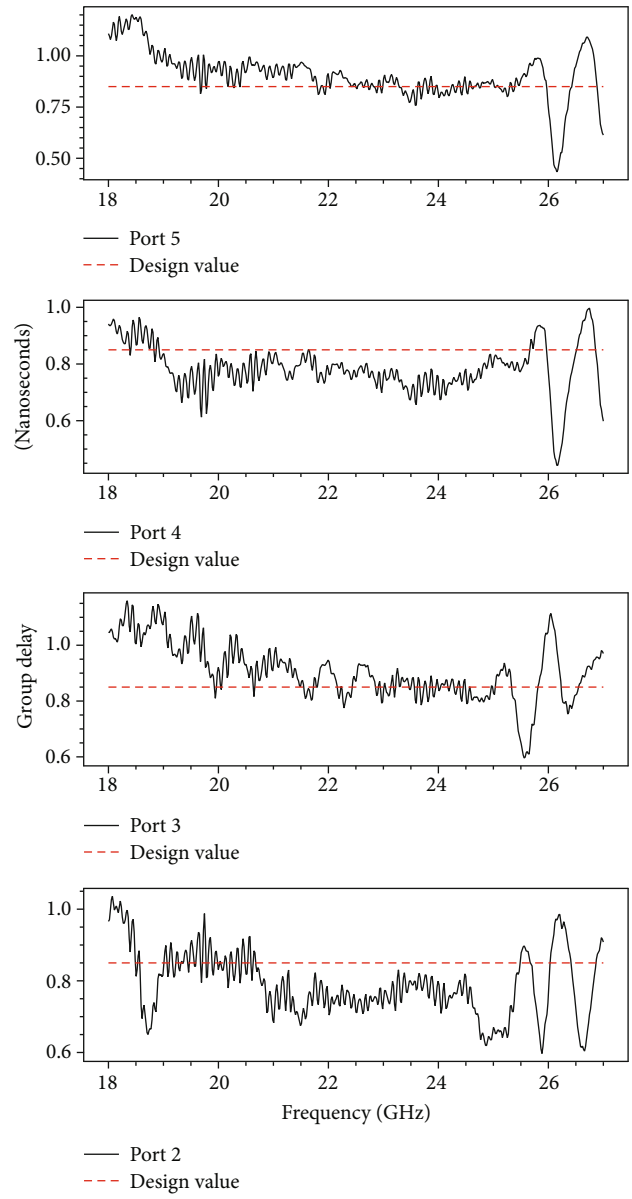

Figure 5: Group delays from the input port to the output ports.

4.1. Feed Network Results. The port parameters of the network are shown in Figure 4. The frequency response is dominated by the response of the power combiners while the time delays and horns had little effect. In all cases, the match was better than −20 dB in the band of 21.5 GHz to 23.5 GHz, which translates to a VSWR of less than 1.22. This makes the array suitable for use in ITU Region 1 for several satcom applications, including the upper channels of the broadcast satellite band at 21.4-22 GHz, the 22.21-22.5 GHz earth exploration satellite band, and both intersatellite bands of 22.55 GHz-23.15 GHz and 23.15 GHz-23.55 GHz. The powers reaching the radiators are all within 1.2 dB of the ideal −6 dB across the band of 21.5-23.5 GHz. This limited operating band is largely a function of the bandwidth of the power dividers. On average, the power is less than −6 dB in the band because of losses in the waveguide. In Figure 5, the group delay of the signals arriving at the horns is shown.

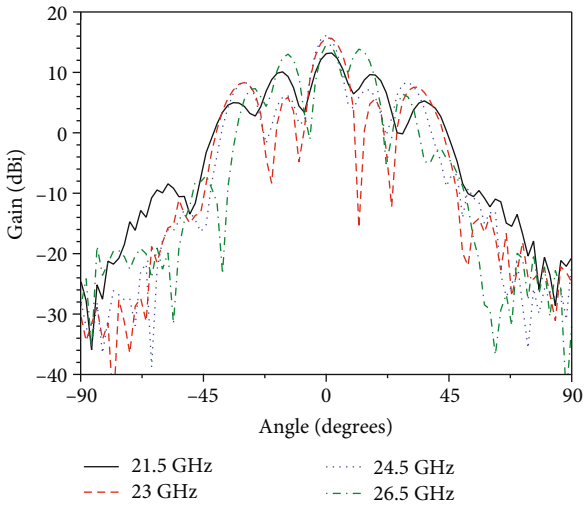

FIGURE 6: Measured copolar pattern for the compensated array.

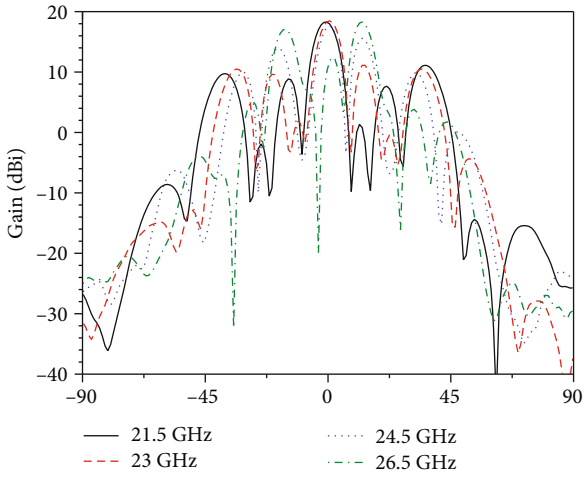

FIGURE 7: Simulated copolar pattern for the compensated antenna array.

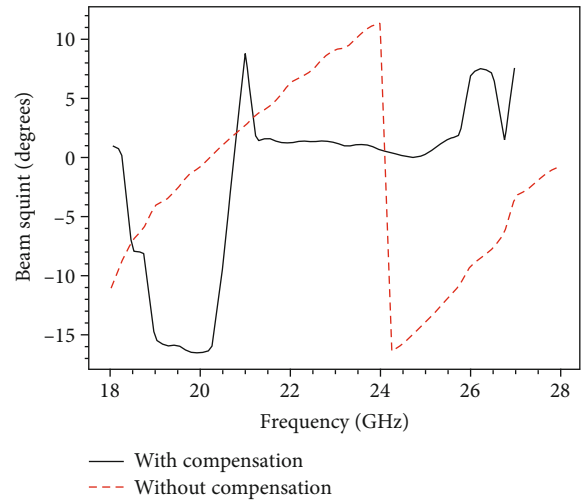

FIGURE 8: Beam squint vs. frequency. The compensated array is compared to the compensated array.

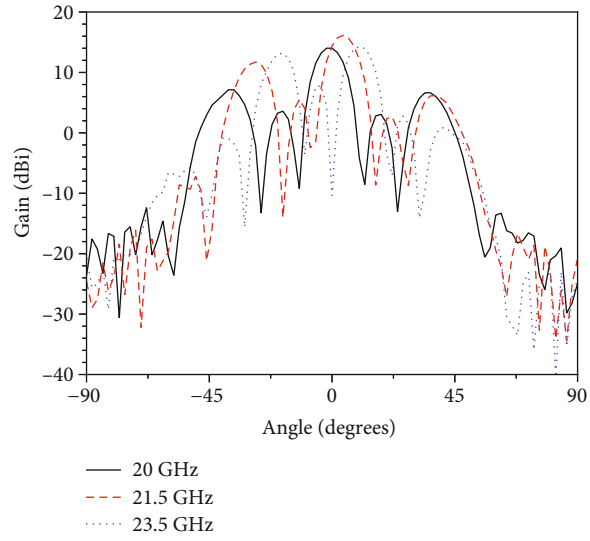

FIGURE 9: Measured copolar pattern for the uncompensated array.

The Figure 5 illustrates the effects of the time delay sections. Despite all paths having different lengths, the group delays are similar within 0.3 ns in the band 21.5-22.5 GHz, resulting in nearly equal phases at the output of the feed network.

4.2. Array Results. The radiation pattern measured in a compact range is shown in Figure 6. The compensated array achieved a peak gain of 15.50 dBi (Figure 6) while the simulated array achieved a gain of 18.85 dBi (Figure 7). The reduced gain can be attributed to loss in the silver plating and accuracy of the SLA printing, with the excess losses in the delay lines ranging from 0.5 to 2.5 dB.

Whereas the main lobe of the array with compensation maintains its direction throughout the band of interest with minor deviation, the uncompensated array exhibits squint throughout the frequency range. Over the band of 21.5-25.5 GHz, the compensated array exhibits less than 1.53° beam steering variation, while the uncompensated beam varies by 10.52° over a similar bandwidth (20-24 GHz) (Figure 8).

The uncompensated array (Figure 9) achieved a peak gain of 14.5 dBi, with the reduced gain attributed to a mismatch in the phases of the waves arriving at the horns. The measured side lobe level (SLL) of the compensated array was 7.30 dBi at 23.5 GHz compared to 8.27 dB in the simulation, with the uncompensated array featuring 6.88 dB SLL at 20 GHz compared to 7.24 dB in the simulation. The low SLL in both designs is a result of uniform excitation amplitude and 1.7 λ_0 array spacing. It further reduces over frequency, reaching 0 dB in places where the grating lobe becomes the main lobe. As expected, the elevation gain in the H-plane (shown in Figure 10) is more consistent over frequency, since there are no horns placed along an axis that would affect the elevation pattern shape.

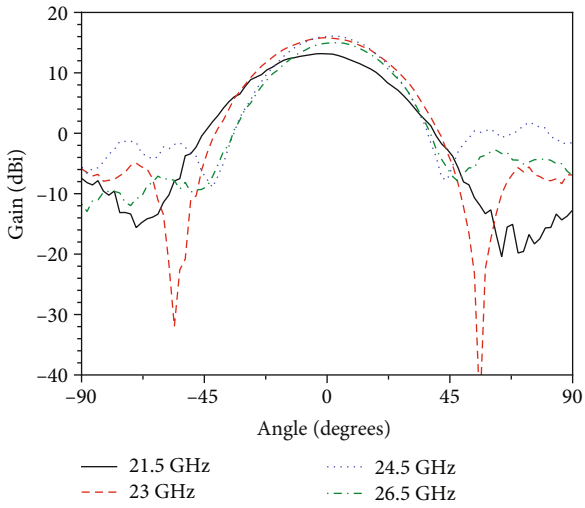

FIGURE 10: Compensated array elevation patterns.

5. Conclusions

Two WR42 series-fed horn antenna arrays were manufactured, with one featuring synthesized delay paths between the feedline and the radiators and the other without this compensation. It is demonstrated that the inclusion of delay equalization reduced the beam squint from 10.52° to 1.53° over a 4 GHz bandwidth at K-band. The bandwidth of the array is further found to be highly dependent on the bandwidth of the time delay sections. Future work will seek to reduce the size of the delay line sections and improve the operating bandwidth of the array even further.

Data Availability

The s2p and antenna pattern data used to support the findings of this study have been deposited in the University of Pretoria's data management platform. The following link can be used to access the repo: https://figshare.com/s/94aa463ae67eb8a75efc.

Conflicts of Interest

The authors declare that there is no conflict of interest regarding the publication of this paper.

Acknowledgments

This work was funded by the National Research Foundation (NRF), South Africa, under grant UID137950 and the University of Pretoria Additive Manufacturing for Electronics Systems grant.

References

[1] H. Mirzaei and G. V. Eleftheriades, "Eliminating beam-squinting in wideband linear series-fed antenna arrays using feed networks constructed by slow-wave transmission lines," *IEEE Antennas and Wireless Propagation Letters*, vol. 15, pp. 798–801, 2016.

[2] H. Mirzaei and G. V. Eleftheriades, "Arbitrary-angle squint- free beamforming in series-fed antenna arrays using non-Foster elements synthesized by negative-group-delay networks," *IEEE Transactions on Antennas and Propagation*, vol. 63, no. 5, pp. 1997–2010, 2015.

[3] M. Longbrake, "True time-delay beamsteering for radar," in *2012 IEEE National Aerospace and Electronics Conference (NAECON)*, vol. 41, pp. 503–506, Dayton, OH, USA, 2012.

[4] H. Mirzaei and G. V. Eleftheriades, "An active artificial transmission line for squint-free series-fed antenna array applications," in *2011 41st European Microwave Conference*, vol. 41, pp. 503–506, Manchester, UK, 2011.

[5] Y. Li and K. M. Luk, "60-GHz substrate integrated waveguide fed cavity-backed aperture-coupled microstrip patch antenna arrays," *IEEE Transactions on Antennas and Propagation*, vol. 63, no. 3, pp. 1075–1085, 2015.

[6] R. Chopra and G. Kumar, "Series-fed binomial microstrip arrays for extremely low sidelobe level," *IEEE Transactions on Antennas and Propagation*, vol. 67, no. 6, pp. 4275–4279, 2019.

[7] J. He, Y. Wu, D. Chen, M. Zhang, J. Hirokawa, and Q. Liu, "Realization of a wideband series-fed 4× 4-element waveguide slot array in the X-band," *IEEE Access*, vol. 9, pp. 83666–83675, 2021.

[8] A. Mehdipour, J. W. Wong, and G. V. Eleftheriades, "Beam-squinting reduction of leaky-wave antennas using Huygens metasurfaces," *IEEE Transactions on Antennas and Propagation*, vol. 63, no. 3, pp. 978–992, 2015.

[9] L. Wang, J. L. Gomez-Tornero, and O. Quevedo-Teruel, "Dispersion reduced SIW leaky-wave antenna by loading metasurface prism," in *2018 International Workshop on Antenna Technology (iWAT)*, pp. 1–3, Nanjing, China, 2018.

[10] J. Long, M. Jacob, and D. F. Sievenpiper, "Electronically steerable antenna using superluminal waveguide and tunable negative capacitors," in *Proceedings of the 2012 IEEE International Symposium on Antennas and Propagation*, pp. 1-2, Chicago, IL, USA, 2012.

[11] M. Kitano, T. Nakanishi, and K. Sugiyama, "Negative group delay and superluminal propagation: an electronic circuit approach," *IEEE Journal of Selected Topics in Quantum Electronics*, vol. 9, no. 1, pp. 43–51, 2003.

[12] S. H. Lee, J. S. Kim, Y. J. Yoon, and W. S. Lee, "Six-way power divider for series feed using H-plane T-junctions," *Microwave and Optical Technology Letters*, vol. 58, no. 7, pp. 1622–1626, 2016.

[13] O. R. Asfar and M. H. Bataineh, "Microwave filter response of nonuniformly corrugated circular waveguide," *Journal of Electromagnetic Waves and Applications*, vol. 9, no. 1–2, pp. 127–143, 1995.

[14] X. Xu, Y. Wei, F. Shen et al., "Sine waveguide for 0.22-THz traveling-wave tube," *IEEE Electron Device Letters*, vol. 32, no. 8, pp. 1152–1154, 2011.

[15] LabsF, "High performance 3D printers," 2022, November, 2022, https://formlabs.com.

[16] J. Shen, M. Aiken, C. Ladd, M. D. Dickey, and D. S. Ricketts, "A simple electroless plating solution for 3D printed microwave components," in *2016 Asia-Pacific Microwave Conference (APMC)*, pp. 1–4, New Delhi, India, 2016.

[17] A. Simonovic, E. Rohwer, and T. Stander, "SLA-printed K-Band waveguide components using Tollens reaction silver plating," *IEEE Trans Compon Packaging Manuf Technol*, vol. 13, no. 2, pp. 230–239, 2023.

[18] A. Simonovic, E. Rohwer, and T. Stander, "Preliminary investigation into the use of silver seed layers in copper electroplating of waveguide parts," in *2022 International Conference on Electromagnetics in Advanced Applications (ICEAA)*, pp. 361–364, Cape Town, South Africa, 2022.